

Tropylium Derivatives as New Entrants that Sense Quadruplex Structures

Daisuke Hori^{1,‡}, Ji Hye Yum^{1,‡}, Hiroshi Sugiyama^{1,2,*}, and Soyoung Park^{1,*}

¹Department of Chemistry, Graduate School of Science, Kyoto University, Kitashirakawa-oiwakecho, Sakyo-ku, Kyoto 606-8502, Japan

²Institute for Integrated Cell-Material Sciences (iCeMS), Kyoto University, Yoshida-ushinomiya-cho, Sakyo-ku, Kyoto 606-8501, Japan



E-mail: <oleesy@kuchem.kyoto-u.ac.jp, hs@kuchem.kyoto-u.ac.jp >

Dr. Soyoung Park, Dr. Prof. Hiroshi Sugiyama

Short Articles: portrait photograph only

Other type publication: portrait photograph and brief biography (within about 100 words)

Portrait photograph and brief biography of the corresponding author(s) and the first author can be published.

Abstract

G-quadruplex (G4) is the most well-known noncanonical conformation of DNA involved in diverse pharmacological and biological contexts. G4 ligands have been actively developed as molecular probes and tumor therapeutic reagent candidates. They have also been used to detect the presence of G4s and identify their biological roles. Currently used ligands are commonly aromatic, planar, and electron deficient for effective interaction with G4s. Recognizing that tropylium cations possess the aforementioned features of effective G4 ligands, we prepared tropylium derivatives to validate their binding affinity with G4s. Titration against various DNA sequences revealed gradual changes in the UV–vis spectra of the tropylium derivatives. A strong hypochromic effect, indicating intercalation or π – π stacking, was observed when *c-kit* DNA was present in a binding ratio of 2:1 (ligand:DNA). The energetically minimized binding model showed that the G4–ligand complexes were stabilized by electrostatic interactions. Encouraged by the present findings, the application of tropylium derivatives in cellular contexts is underway.

Keywords: G-quadruplex, Quadruplex ligand, Tropylium cations

1. Introduction

Structural heterogeneity is an intrinsic property of nucleic acids and is directly linked to gene regulation.¹ Identification of a wide variety of structural motifs in cells is a crucial step in understanding their function and regulatory mechanisms. Therefore, great effort has been made in developing structure profiling techniques including isomorphous fluorescent nucleosides², ¹⁹F-labeled nucleosides³, and antibodies⁴. Thanks to these useful tools, the presence of noncanonical structures and their roles have been revealed. Among the various structural motifs, G-quadruplexes (G4s) are one of the most noteworthy noncanonical conformations and are constructed from layers of G-tetrad DNA^{5,6}. With the development of G4 ligands, researchers have begun to unravel the functions of G4s in nuclei. For example, G4 DNA has profound implications in biological events such as telomere regulations⁷, controls of gene expression⁸, and cellular phase separation⁹. G4 ligands belong to a class of compound that selectively binds to G4s and interferes with their further interactions (Figure 1A). Many of the current generations of G4 ligands have the common properties of (1)

structural planarity, (2) a large conjugated system of p-orbital electrons, and (3) partial positive charge¹⁰. Currently, a large number of G4 ligands have been designed and evaluated as molecular chemical probes and therapeutic reagents¹¹.

Tropylium cation is a cationic seven-member aromatic ring that has been used as a versatile reactant and catalyst for various organic reactions. For example, Nguyen and coworkers have been involved in expanding the applicability of tropylium cations. They have reported the catalysis of nucleophilic substitutions, oxidative alpha-additions, carbonyl–olefin metathesis, and hydration reactions by tropylium cations^{12,13}. Owing to its versatility, tropylium has been used in both flow- and batch-chemistry setups¹⁴. The acetalization of aldehydes, prenylation of phenols, and C–C bond cleavage reactions have been carried out via flow reactor with tropylium cations. Recently, new organic dyes bearing tropylium structures have also been developed¹⁵. A set of electron-donating anilines was conjugated on tropylium to obtain push–pull-type molecules, and their chromatic characteristics and fluorescent properties under differing solvent conditions were explored. Depending on anion coordination, these molecules react sensitively and display different colors or fluorescence, suggesting potential use as molecular probes.

Interestingly, the tropylium moiety shows attractive features associated with the abovementioned G4 ligands: planarity, aromaticity, and electrophilicity. Based on these features, here we explored the potential of tropylium derivatives as G4-binding ligands. After identifying solvent effects, we evaluated the binding ability of tropylium derivatives to various DNA secondary structures via UV titration assays. The UV–vis spectra clearly demonstrated that selective binding of tropylium derivatives to G4s was achieved through π – π interaction, and this observation was supported by molecular modeling studies.

2. Experimental

Methods and Equipment

NMR spectra were obtained using a JEOL JNM ECA-600 spectrometer operating at 600 MHz for ¹H NMR and 150 MHz for ¹³C NMR in CDCl₃ unless otherwise noted. Flash column chromatography was performed employing Silica Gel 60 (70–230 mesh, Merck Chemicals). Silica-gel preparative thin-layer chromatography was performed using plates of silica gel 70 PF₂₅₄ (Wako Pure Chemical Ind. Ltd.). DNA concentrations were measured by a NanoDrop ND-1000 spectrophotometer

(NanoDrop Technologies, Wilmington, DE). Stock 100 mM Na cacodylate buffer (pH 5.5, pH 7.0) and Tris-HCl buffer (pH 7.5) were prepared by dissolving sodium cacodylate trihydrate (1.07 g, 5.0 mmol) or trisaminomethane base (1.21 g, 5.0 mmol) in milliQ water (25 mL) before adjusting to the desired pH with hydrochloric acid and minimal sodium hydroxide, then topping up to 50 mL with milliQ water. pH was measured using a LAQUA F-72 pH/ion meter (HORIBA Ltd., Kyoto, Japan).

Synthesis of Tropylium Derivatives

The synthesis of tropylium derivatives (**4a-4d**) was carried out by mixing NaH-activated aniline motifs (**2a-2d**) with 1 equivalent of tropylium tetrafluoroborate in ACN. The corresponding intermediates (**3a-3d**) of tropylium salts were obtained in excellent yield (~80%), and subsequent oxidative hydride abstractions were performed to generate final products. To get Trop-AzP (**4d**), additional synthetic step to prepare 1-phenylazetidene was conducted via Buchwald-Hartwig coupling reaction. The precursor was obtained in good yield (50%) and applied for tropylium conjugation reaction.

Oligonucleotide Synthesis

Oligonucleotides (ODNs) were synthesized on solid supports using commercially available *O*^{5'}-dimethoxytrityl-2'-deoxyribonucleoside *O*^{3'}-phosphoramidites. Solid-phase ODN synthesis was performed on an ABI DNA synthesizer (Applied Biosystem, Foster City, CA). Cleavage from the solid support and deprotection was accomplished with 50:50 of MeNH₂ in 40 wt.% in water and NH₃ in 28 wt.% in water at room temperature (RT) for 15 min and then at 65 °C for 15 min. The synthesized ODNs were eluted from Glen-Pak™ DNA purification cartridges with purification steps performed as per the procedure. The final elution was subjected to normal-phase HPLC purification for the quality check. The products were confirmed by MALDI-TOF MS using a Bruker microflex-KSII (Bruker Corporation, Billerica, MA) (Table S2). DNA concentrations were determined using the NanoDrop ND-1000.

Solvatochromism of Tropylium Derivatives

Synthesized tropylium derivatives (both known and newly synthesized ones) were prepared as a stock solution (5 mM in DMSO). For spectroscopic studies, samples were prepared by dissolving tropylium derivatives in various solvents (MeOH, water, acetonitrile, ethyl acetate, dichloromethane, and dichloroethane) or acetonitrile in the presence of 1.0 equivalent of TBAF, TBAC, TBAB, or TBAI to 50 μM. UV-vis absorbance spectra were measured from 220 nm to 700 nm at 20 °C on a JASCO V-750 spectrophotometer equipped with a JASCO PAC-743R thermocontrolled cell changer and a JASCO CTU-100 thermocirculator.

UV titration

Binding assays were performed with pre-formed DNAs under corresponding buffer conditions. All ODNs were dissolved in the required buffer at the indicated concentration. The solution was first heated to 95 °C for 5 min and then cooled slowly to RT over a period of 6 h. The ligand solution (50 μM, 500 μL) was titrated by stepwise addition of aliquots of the DNA solution (1.5 mM). 20 mM Na cacodylate (pH 7.0) with 100 mM NaCl for duplex DNA titration, 20 mM Na cacodylate (pH 5.5) for i-motif DNA titration, and 20 mM Na cacodylate (pH 7.0) with 100 mM KCl for G4 DNA titration were prepared. After each DNA addition, the mixture was incubated at 20 °C for 5 min before measurement.

CD Spectroscopy and Melting measurement

CD spectra of ODN solutions collected in 1 nm steps from 360 nm to 220 nm were measured using a JASCO J-805LST spectrometer in a 1 cm quartz cuvette. The samples were denatured at 95 °C for 5 min and annealed slowly to RT until experiments were initiated. All samples were prepared in a total volume of 120 μL containing 4 μM ODN in the presence of tropylium derivatives under certain secondary structure-forming conditions. For melting measurements, ellipticity was recorded in the forward direction at temperatures from RT to 95 °C at a rate of 1.0 °C/min. Each spectrum shown is the average of two individual scans.

Cytotoxicity

Cultured HeLa cells were purchased from ATCC and maintained in DMEM (Thermo Fisher Scientific) supplemented with 10% (v/v) fetal bovine serum (FBS, Sigma Aldrich) at 37 °C with 5% CO₂. For the compound treatment, cells were seeded in a 96-well plate (ca. 5000 cells/well). Cultures were maintained at 37 °C in a humidified atmosphere containing 5% CO₂. After 2 days of incubation to promote cell adhesion, cells were incubated overnight with the tropylium derivatives at 10 μM, 1 μM, and 0.1 μM (0.5% v/v). Wells containing 0.5% (v/v) DMSO without cells were used as control. At the end of incubation, Cell Count Reagent SF (from Nacalai Tesque Inc.) was added to the cell culture medium 10% (v/v) and incubated for 1 h at 37 °C. Finally, the absorbance was recorded in a SpectraMax M2 microplate reader (Molecular Devices) at 450 nm. Cell viability relative to control was expressed as mean ± SEM from at least three different experiments.

ITC Measurements

ITC experiments were performed on formed DNAs using a MicroCal™ iTC200 isothermal titration calorimeter courtesy by prof. Takashi Morii and Dr. Eiji Nakata. The titration of 2 mM Trop-DEA on 10 μM duplex, c-kit G4, and i-motif DNAs was carried out in buffers for secondary structural formation at 25 °C. The titrations were conducted in time interval as 180 s, and the injection volume was 2.0 μL. The reference cell contained distilled and deionized water. Before the experiment, the samples were heated at 95 °C, 5 min then slowly cooled down to RT (1 °C min⁻¹). The data were analyzed using Origin 7.0 (Microcal software) with an automatically generated baseline.

DFT Calculations

The geometry of tropylium derivatives are optimized using DFT in the Gaussian 16W program package. The molecules were prepared with Gaussian View software, and calculation setup was based on the previous report.¹⁵ All the calculations are done using B3LYP (Becke, three-parameter, Lee-Yang-Parr) hybrid exchange and correlation energy functional, ground state, default spin, with the 6-311G+(d,p) basis set for all atoms. After geometry optimization, frequency calculations are done to remove any vibrational unstable mode in gas state.

Molecular Modeling study

Molecular modeling between DNA and ligands was carried out using the DS (Discovery Studio Client 2019) software package. The c-kit G-quadruplex DNA has prepared base on previously reported crystal structure (PDB ID: 2O3M). The structure optimized tropylium derivatives were positioned to the designated G-quartet of c-kit. For the construction of environment components before the minimization, the solvation step was conducted in the presence of KCl. Minimizations (RMS Gradient to be 0.001) were operated for each model with CHARMM force field parameters.

3. Results

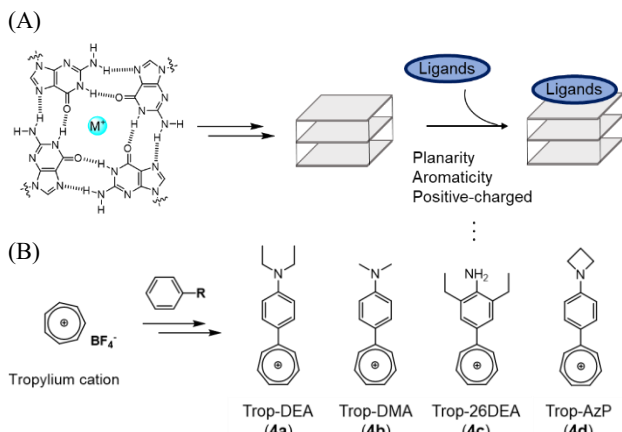


Figure 1. Tropylium derivatives as new G-quadruplex ligand candidates

(A) Schematic representation of G-quadruplex and G-quadruplex ligands, and (B) tropylium derivatives used in this study.

The structures of ligands used in this study are shown in Figure 1B. Following a previously reported synthetic procedure¹⁵, tropylium derivatives bearing a large π -conjugation system (**4a–4d**) were synthesized. For the DNA binding study, we newly designed Trop-AzP (**4d**) containing a strong electron-donating azetidine moiety. For the preparation of **4d**, azetidine hydrochloride and iodobenzene were coupled via the Buchwald–Hartwig amination¹⁶. Subsequently, tropylium tetrafluoroborate was added and para-substituted on the benzene ring. All of the compounds were obtained in good to excellent yield (yield 50%–92%), and identified with NMR and ESI–MS (see SI). As conventional tropylium derivatives have shown a solvation effect, we also validated the solvent effect of the newly synthesized Trop-AzP (Figure 2 and Figures S4–S5). Compared with other tropylium derivatives, Trop-AzP exhibited low molar absorptivity in various solvents. Its absorption and emission maxima varied between 520–590 nm and 470–550 nm ($\lambda_{\text{ex}} = 365$ nm), respectively, depending on the solvent. Consistent with a previous report¹⁵, we observed the weakest absorption in water and the strongest emission in ethyl acetate (Figure 2, see SI for broader range data). In addition, given the ability of tropylium moieties to coordinate variedly to counterions, spectral profiles of Trop-AzP in the presence of halide anions were investigated. The sample solutions of Trop-AzP (150 μM) were prepared with the same equivalent of tetrabutylammonium halide (TBAX, here $X = \text{F}^-$, Cl^- , Br^- , and I^-). The presence of fluoride ion (F^-) induced strong fluorescence in acetonitrile. It was also observed with the other tropylium ligands as shown in Figure S8. This remarkable fluoride sensitivity and selectivity of tropylium derivatives supports a potential usage of our ligands as fluorescent turn-on probes upon direct bond formation with fluoride ions.¹⁷

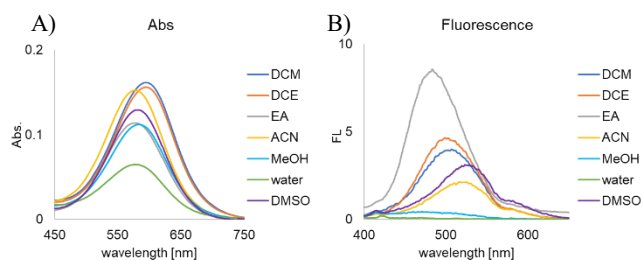


Figure 2. The solvent effect of Trop-AzP

(A) Absorption spectra, and (B) emission spectra ($\lambda_{\text{ex}} = 365$ nm).

Table 1. DNA library for the spectral titrations

duplex	GGACCGCGGTCC
i-motif	CCCTTACCCTTACCCTTACCC
interG4	TTAGGGG
HT22	AGGGTTAGGGTTAGGGTTAGGG
c-kit	AGGGAGGGCGCTGGGAGGAGGG

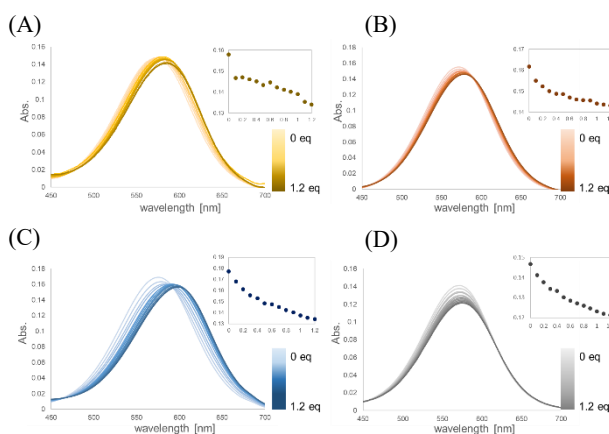


Figure 3. The UV–vis titration spectra of Trop-DEA upon stoichiometric pre-formed DNA addition^a

(A) Duplex DNA (20 mM Na cacodylate pH 7.0, 100 mM NaCl), (B) i-motif DNA (20 mM Na cacodylate pH 5.5), (C) intermolecular G4 (TTAG₄) DNA (20 mM Na cacodylate pH 7.0, 100 mM KCl), and (D) HT22 DNA (20 mM Na cacodylate pH 7.0, 100 mM KCl).

^a Absorption values reflect absorption for 10 μM of ligand.

After characterization of the ligands, the interaction of tropylium derivatives with various DNA secondary structures was examined by UV–vis absorption spectral titrations. To construct the DNA library, we prepared five different DNA sets including canonical duplex DNA, i-motif¹⁸, intermolecular G4¹⁹, and intramolecular G4s²⁰ (Table 1). The experimental parameters and sample preparation for the titration assays are presented in the Supplemental Information (SI). The obtained UV–vis spectra were presented as absorbance per 10 μM for comparison. As shown in Figure 2A, the absorption of ligands is slightly differed, for example, Trop-AzP showed relatively weak absorbance compared with conventional derivatives. For this reason, we presented absorbance per 10 μM to compare degree of spectral changes. We first evaluated Trop-DEA, which exhibited a distinctive absorption spectrum ($\lambda_{\text{max}} = 570$ nm) between 450 nm and 700 nm in water, for the stoichiometric DNA titrations. In all cases, a bathochromic shift (4–27 nm) was observed upon addition of DNA to the sample solution. As the equivalence of the G4s increased, hypochromic effects were also observed. It is known that intercalation or π – π stacking of ligands with DNA causes a hypochromic effect in absorption spectra²¹. The addition of unimolecular HT22, which forms hybrid structures in the presence of potassium ions, induced

strong hypochromicity (Figure 3D), and a similar tendency was obtained with intermolecular parallel G4 (Figure 3C). When we used i-motif for the assay, the constant absorption reduce was observed. The plot chart of i-motif DNA also displayed similar tendency with G4 DNAs (Figure 3B). By contrast, absorption intensity remained relatively unchanged with duplex DNA addition (Figure 3A). Although we anticipated that the ligand would emit fluorescence when interacting with G-quartets, emission was not induced in the presence of the G4 DNA sequence (Figure S7).

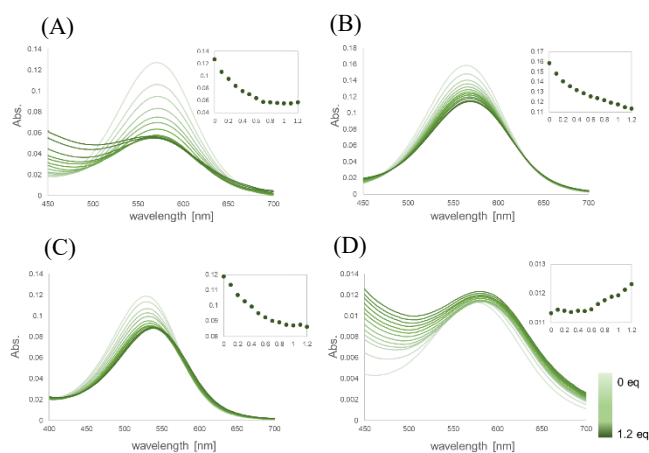


Figure 4. The UV-vis titration spectra of tropylium derivatives upon stoichiometric *c-kit* oligonucleotide addition^a (A) Trop-DEA, (B) Trop-DMA, (C) Trop-26DEA, and (D) Trop-AzP^b.

^a Absorption values reflect absorption for 10 μM of ligand.

^b UV titration measured with 100 μM of the ligand.

Surprisingly, Trop-DEA displayed distinguishable behavior in the presence of *c-kit* DNA. We observed an enhanced hypochromic effect in its titration spectra, indicating a strong interaction between Trop-DEA and *c-kit* G4 (Figure 4A). The plot of λ_{max} (571 nm) showed saturation from 0.5 equivalent of DNA addition, implying a 2:1 (ligand:DNA) interaction model. Inspired by dramatic absorption changes, we quantified the binding affinity between DNAs and the tropylium derivative via isothermal titration calorimetry (Figure S9 and Table S3).²² The enthalpy driven bindings were measured and the binding constants for *c-kit* G4 and i-motif DNA are $8.7 \times 10^3 (\pm 1.03 \times 10^3)$ and $1.4 \times 10^4 (\pm 1.15 \times 10^3)$, respectively. Consistent with UV titration results, duplex DNA did not show interaction with Trop-DEA. CD spectra and UV-melting experiments were also conducted on the tropylium ligand-DNA complexes. In the presence of ligands, a stable parallel structure was maintained, and a slight increase of T_m value (up to 4 $^\circ\text{C}$) was achieved (Figures S10-S12). Based on the spectroscopic studies, we deduced that electrostatic π - π interaction was formed between the ligand and *c-kit* oligomer²¹. Encouraged by the titration result of Trop-DEA with *c-kit* DNA, we investigated the G4 binding abilities of other tropylium derivatives. Likewise, a significant decrease in intensity was detected when we examined Trop-DMA (Figure 4B) and Trop-26DEA (Figure 4C), implying the ligands bind G4 with a similar interaction mode as Trop-DEA (4a). By contrast, despite its weak absorption in water, a hyperchromic shift (Figure 4D) coupled with a blue shift was observed in the case of Trop-AzP (4d). Unlike the other tropylium derivatives, the nonplanar azetidine skeleton of Trop-AzP may make it difficult for the ligand to interact with G-tetrads. To further investigate the binding model, plots of the absorption

maxima of each ligand were recorded. Similar to Trop-DEA, the stoichiometric ratio of ligand to G4 was found to be 2:1 for Trop-26DEA, whereas a continuous decrease in absorption was observed for Trop-DMA.

Our molecular modeling study afforded a plausible binding mode between the ligands and *c-kit* G4. We chose Trop-DEA and G4 complex to develop the molecular model. First, DFT calculation with the G4 ligand was conducted to produce the optimal energy minimized structure (Figures S14-S17). Next, the tropylium derivative was positioned on both sides of G-tetrads (Ligand:DNA = 2:1), then this cooperative complex was structurally minimized. The minimized structure, a stable 2:1 complex, included two Trop-DEA ligands well-fitted to the G4 by favorable stacking, and is supportive of cooperative interaction between the ligands and G4 (Figure S18).

4. Discussion and Conclusion

Attracted by the various features of tropylium ions, their ability to interact with DNAs was explored in this study. Along with the conventional tropylium derivatives, we newly designed azetidylphenyl-containing Trop-AzP in this study. We demonstrated that our ligand candidates were highly water soluble, visible light absorbing, and sensitive to the surroundings; the tropylium derivatives exhibited diverse colorimetric responses depending on the solvent environment. In addition, these compounds interacted with various quadruplexes as supported by their titration spectra. Upon the addition of quadruplex DNA sequences, redshifts (4–27 nm) and hypochromicity (up to 36%) of the absorption maxima were observed. Among validated DNA sets, we found that tropylium derivatives displayed the strong hypochromic effect to *c-kit* DNA. The plots upon stoichiometric *c-kit* oligomer addition provide information on the interaction ratio between the ligands and G4. Trop-DEA and Trop-26DEA showed a 2:1 ligand:DNA ratio consistent with the behavior of well-explored G4 ligands. Unexpectedly, newly synthesized Trop-AzP (4d) was unable to coordinate to *c-kit* DNA. Since tropylium derivatives are examined as the quadruplex binding ligands for the first time, we moved to quantify the binding affinity toward DNA sets. An isothermal titration calorimetry has been used for obtaining binding constants between DNAs and Trop-DEA. The duplex DNA, i-motif DNA, and *c-kit* G4 were employed for ligand titrations. I-motif and G-quadruplex DNA showed moderate binding affinity with Trop-DEA compared with conventional G-quadruplex ligands.²³ The data resulted in negative enthalpy (ΔH) of interaction value at 25 $^\circ\text{C}$, meaning all enthalpically favored complexes formations. Also, we obtained negative value of free energy (ΔG) in both cases. Continuously focusing on the diethyl-modified derivatives, we performed a molecular modeling study to predict the overall structures and binding models. The parallel *c-kit* G4 has open G-tetrads at both the top and the bottom faces, and where the two equivalents of Trop-DEA and Trop-26DEA were located. After minimizing the structure, we obtained well-stacked and stable complexes coordinated through electrostatic interactions. Altogether, we demonstrated that tropylium derivatives function as quadruplex ligands.

Distinct from the conventional G4 ligand skeletons (porphyrins, polyacenes, thioflavins, etc.)^{21,24}, we propose tropylium derivatives as new structural motifs and successfully demonstrate its quadruplex-specific binding abilities. Compared with other reported ligands, tropylium derivatives possess the following advantages: small size (MW. ~ 300), facile synthesis (two steps with excellent yield), and high solubility in aqueous conditions. The interaction mode of the ligands was proposed based on a molecular modeling study conducted under reproducible conditions. We plan to further investigate the exact

configuration and binding model of DNA–ligand complexes by both NMR studies and crystallography²⁵. Given the prevalence of use of quadruplex ligands in therapeutic and detection purposes¹¹, these tropylium derivatives have the potential to be exploited using cell studies *in vitro*. For instance, additional functionalization of the current tropylium derivatives would enable the molecules to emit strong fluorescence for cellular imaging *in vivo*. To that end, we performed a cytotoxicity assay with HeLa cells (Figure S13), which indicated that high cell viability was maintained in the presence of the tropylium derivatives. The G4-containing promoter sequences, which displays interaction with our ligands, could be next our target for chemical biology applications²⁶. For instance, investigation of the regulation of expression of the *c-kit* promoter region in *c-kit*-associated cancer cells with our ligands is underway.

Associated content

Synthetic routes and characterization data of new tropylium derivative, HPLC data, ESI-TOF-Mass data, spectroscopic data of oligonucleotides. This material is available free of charge via the Internet at <http://pubs.acs.org>.

Note

The authors declare no competing financial interest.

Acknowledgement

We express sincere thanks for a Grant-in-Aid Priority Research (16H06356 for H. S) from Japan Society for the Promotion of Science (JSPS). We also thank KAKENHI program (Grant-in-Aid for scientific research C, 18K05315) and Research Encouragement Grant from The Asahi Glass Foundation for support to S. P. We like to thank Prof. Takashi Morii and Associate Prof. Eiji Nakata for assistance to measure isothermal titration calorimetry. We are thankful to lovely Wen Ann Wee for English correction.

References

- (1) a) S. De, F. Michor, *Nat. Struct. Mol. Biol.* **2011**, *18*(8), 950.; b) H. Sugiyama, *Bull. Chem. Soc. Jpn.* **2007**, *80*(5), 823-841.; c) N. Sugimoto, *Bull. Chem. Soc. Jpn.* **2009**, *82*(1), 1-10.
- (2) a) R. W. Sinkeldam, N. J. Greco, Y. Tor, *Chem. Rev.* **2010**, *110*(5), 2579-2619.; b) A. Podder, H. J. Lee, B. H. Kim, *Bull. Chem. Soc. Jpn.* **2021**, DOI: 10.1246/bcsj.20200351.; c) S. Park, H. Otomo, L. Zheng, H. Sugiyama, *Chem. Commun.* **2014**, *50*, 1573-1575.; d) S. Yamamoto, S. Park, H. Sugiyama, *RSC Adv.* **2015**, *5*(126), 104601-104605.; e) T. Zhou, Y. Wang, X. Li, Q. Zhang, T. Li, *Bull. Chem. Soc. Jpn.* **2006**, *79*(8), 1300-1302.
- (3) a) S. Nakamura, H. Yang, C. Hirata, F. Kersaudy, K. Fujimoto, *Org. Biomol. Chem.* **2017**, *15*, 5109-5111.; b) F. Nagatsugi, K. Onizuka, *Chem. Lett.* **2020**, *49*(7), 771-780.; c) S. Manna, D. Sarkar, S. G. Srivatsan, *J. Am. Chem. Soc.* **2018**, *140*, 12622-12633.; d) S. L. Cobb, C. D. Murphy, *J. Fluor. Chem.* **2009**, *130*(2), 132-143.
- (4) a) G. Biffi, D. Tannahill, J. McCafferty, S. Balasubramanian, *Nat. Chem.* **2013**, *5*(3), 182-186.; b) H. J. Lipps, D. Rhodes. *Trends Cell Biol.* **2009**, *19*(8), 414-422.; c) E. M. Lafer, A. Möller, A. Nordheim, B. D. Stollar, A. Rich, *Proc. Natl. Acad. Sci. U. S. A.* **1981**, *78*(6), 3546-3550.; d) M. Komiyama, K. Yoshimoto, M. Sisido, K. Ariga, *Bull. Chem. Soc. Jpn.* **2017**, *90*(9), 967-1004.
- (5) a) M. Gellert, M. N. Lipsett, D. R. Davies, *Proc. Natl. Acad. Sci. U. S. A.* **1962**, *48*, 2013-2018.; b) D. Sen, W. Gilbert, *Nature* **1988**, *334*, 364-366.; c) J. L. Huppert, *FEBS J.* **2010**, *277*, 3452-3458.; d) H. Shimizu, H. Tai, K. Saito, T. Shibata, M. Kinoshita, Y. Yamamoto, *Bull. Chem. Soc. Jpn.* **2015**, *88*(5), 644-652.
- (6) [For review] a) J. L. Mergny, D. Sen, *Chem. Rev.* **2019**, *119*, 6290-6325.; b) A. T. Phan, V. Kuryavyi, D. J. Patel, *Curr. Opin. Struct. Biol.* **2006**, *16*, 288-298.; c) S. Asamitsu, S. Obata, Z. Yu, T. Bando, H. Sugiyama, *Molecules* **2019**, *24*(3), 429.; d) D. Yang, C. Lin, eds., *G-Quadruplex Nucleic Acids: Methods and Protocols.* **2019**, Humana Press.
- (7) a) D. Sun, B. Thompson, B. E. Cathers, M. Salazar, S. M. Kerwin, J. O. Trent, T. C. Jenkins, S. Neidle, L. H. Hurley, *J. Med. Chem.* **1997**, *40*, 2113-2116.; b) R. T. Wheelhouse, D. Sun, H. Han, F. X. Han, L. H. Hurley, *J. Am. Chem. Soc.* **1998**, *120*, 3261-3262.
- (8) a) D. Rhodes, H. J. Lipps, *Nucleic Acids Res.* **2015**, *43*(18), 8627-8637.; b) D. Ren'ciuk, J. Ryneš, I. Kejnovská, S. Foldynová-Trantírková, M. Andäng, L. Trantírek, M. Vorlíčková, *Biochim. Biophys. Acta (BBA) Gene Regul. Mech.* **2017**, *1860*, 175-183.; c) M. L. Bochman, K. Paeschke, V. A. Zakian, *Nat. Rev. Genet.* **2012**, *13*(11), 770-780.
- (9) a) S. Asamitsu, Y. Yabuki, S. Ikenoshita, K. Kawakubo, M. Kawasaki, S. Usuki, Y. Nakayama, K. Adachi, H. Kugoh, K. Ishii, T. Matsuura, *Sci. Adv.* **2021**, *7*(3), eabd9440.; b) P. A. Chong, R. M. Vernon, J. D. Forman-Kay, *J. Mol. Biol.* **2018**, *430*(23), 4650-4665.; c) S. Asamitsu, N. Shioda, *J. Biochem.* **2021**, DOI: 10.1093/jb/mvab018
- (10) a) D. Monchaud, M. P. Teulade-Fichou, *Org. Biomol. Chem.* **2008**, *6*(4), 627-636.; b) S. Asamitsu, T. Bando, H. Sugiyama, *Chem. Eur. J.* **2019**, *25*(2), 417-430.; c) H. Yaku, T. Fujimoto, T. Murashima, D. Miyoshi, N. Sugimoto, *Chem. Commun.* **2012**, *48*(50), 6203-6216.
- (11) a) S. Neidle, *J. Med. Chem.* **2016**, *59*(13), 5987-6011.; b) D. L. Ma, Z. Zhang, M. Wang, L. Lu, H. J. Zhong, C. H. Leung, *Chem. Biol.* **2015**, *22*(7), 812-828.; c) S. Neidle, *The FEBS J.* **2010**, *277*(5), 1118-1125.
- (12) a) Z. N. Parnes, M. E. Volpin, D. N. Kursanov, *Tetrahedron Lett.* **1960**, *1*(42), 20-23.; b) T. V. Nguyen, M. Hall, *Tetrahedron Lett.* **2014**, *55*(50), 6895-6898.; c) T. V. Nguyen, D. J. Lyons, *Chem. Commun.* **2015**, *51*(15), 3131-3134.; d) G. Oss, S. D. de Vos, K. N. Luc, J. B. Harper, T. V. Nguyen, *J. Org. Chem.* **2018**, *83*(2), 1000-1010.
- (13) a) X. Shao, L. Tian, Y. Wang, *Eur. J. Org. Chem.* **2019**, *2019*(25), 4089-4094.; b) U. P. Tran, G. Oss, D. P. Pace, J. Ho, T. V. Nguyen, *Chem. Sci.* **2018**, *9*(23), 5145-5151.; c) M. A. Hussein, U. P. Tran, V. T. Huynh, J. Ho, M. Bhadbhade, H. Mayr, T. V. Nguyen, *Angew. Chem. Int. Ed.* **2020**, *59*, 1455-1459.; d) C. Empel, T. V. Nguyen, R. M. Koenigs, *Org. Lett.* **2021**, *23*(2), 548-553.
- (14) a) K. Omoregbee, K. N. Luc, A. H. Dinh, T. V. Nguyen, *J. Flow. Chem.* **2020**, *10*(1), 161-166.; b) M. A. Hussein, V. T. Huynh, R. Hommelsheim, R. M. Koenigs, T. V. Nguyen, *Chem. Commun.* **2018**, *54*(92), 12970-12973.; c) D. J. M. Lyons, R. D. Crocker, D. Enders, T. V. Nguyen, *Green Chem.* **2017**, *19*(17), 3993-3996.
- (15) D. J. M. Lyons, R. D. Crocker, T. V. Nguyen *Chem. Eur. J.* **2018**, *24*(43), 10959-10965.
- (16) a) S. J. Siegl, J. Galeta, R. Dzijak, A. Vázquez, M. Del Río-Villanueva, M. Dračinský, M. Vrabec, *ChemBioChem*, **2019**, *20*(7), 886.; b) S. M. Crawford, C. A. Wheaton, V. Mishra, M. Stradiotto, *Can. J. Chem.* **2018**, *96*(6), 578-586.
- (17) a) A. Dhillon, M. Nair, D. Kumar, *Anal. Methods* **2016**, *8*(27), 5338-5352.; b) E. Nakata, Y. Yukimachi, Y. Uto, H. Hori, T. Morii, *Bull. Chem. Soc. Jpn.* **2015**, *88*(2), 327-329.; c) X. Yang, F. Zhu, Y. Li, M. Yan, Y. Cui, G. Sun, *Bull. Chem. Soc. Jpn.* **2020**, *93*(7), 870-879.
- (18) a) J. R. Williamson, *Ann. Rev. Biophys. Biomol. Struct.* **1994**, *23*(1), 703-730.; b) A. T. Phan, J. L. Mergny, *Nucleic Acids Res.* **2002**, *30*(21), 4618-4625.
- (19) a) M. Kinoshita, S. Takaya, T. Shibata, H. Hemmi, Y. Yamamoto, *Chem. Lett.* **2015**, *44*(8), 1107-1109.; b) Y. Kato, T. Ohyama, H. Mita, Y. Yamamoto, *J. Am. Chem. Soc.*

2005, 127(28), 9980-9981.; c) M. Uchiyama, A. Momotake, T. Ikeue, Y. Yamamoto, *Bull. Chem. Soc. Jpn.* **2020**, 93(12), 1504-1508.

(20) A. T. Phan, V. Kuryavyi, S. Burge, S. Neidle, D. J. Patel, *J. Am. Chem. Soc.* **2007**, 129(14), 4386-4392.

(21) a) F. X. Han, R. T. Wheelhouse, L. H. Hurley, *J. Am. Chem. Soc.* **1999**, 121(15), 3561-3570.; b) K. Bhadra, G. S. Kumar, *Biochim. Biophys. Acta* **2011**, 1810, 485-496.; c) C. Wei, G. Jia, J. Yuan, Z. Feng, c. Li, *Biochemistry* **2006**, 45(21), 6681-6691.; d) K. Hayasaka, T. Shibata, A. Sugahara, A. Momotake, T. Matsui, S. Neyu, T. Ishizuka, Y. Xu, Y. Yamamoto, *Bull. Chem. Soc. Jpn.* **2020**, 93(5), 621-629.

(22) I. Haq, J. O. Trent, B. Z. Chowdhry, T. C. Jenkins, *J. Am. Chem. Soc.* **1999**, 121, 1768-1779.

(23) B. Pagano, C. A. Mattia, C. Giancola, *Int. J. Mol. Sci.* **2009**, 10(7), 2935-2957.

(24) a) V. Gabelica, R. Maeda, T. Fujimoto, H. Yaku, T. Murashima, N. Sugimoto, D. Miyoshi, *Biochemistry* **2013**, 52(33), 5620-5628.; b) S. Müller, S. Kumari, R. Rodriguez, S. Balasubramanian, *Nat. Chem.* **2010**, 2, 1095-1098.; c) A. De Cian, E. DeLemos, J. L. Mergny, M.-P. Teulade-Fichou, D. Monchaud, *J. Am. Chem. Soc.* **2007**, 129, 1856-1857.; d) Z. Ou, Z. Feng, G. Liu, Y. Chen, Y. Gao, Y. Li, X. Wang, *Chem. Lett.* **2015**, 44(4), 425-427.

(25) a) M. Adrian, F. R. Winnerdy, B. Heddi, A. T. Phan, *Biophys. J.* **2017**, 113(4), 775-784.; b) S. M. Haider, S. Neidle, G. N. Parkinson, *Biochim.* **2011**, 93(8), 1239-1251.; c) P. Murat, Y. Singh, E. Defrancq, *Chem. Soc. Rev.* **2011**, 40(11), 5293-5307.

(26) a) A. P. Rankin, J. Reszka, M. Huppert, G. N. Zloh, A. K. Parkinson, S. Todd, S. Ladame, S. Balasubramanian, S. Neidle, *J. Am. Chem. Soc.* **2005**, 127, 10584-10589.; b) H. Fernando, A. P. Reszka, J. Huppert, S. Ladame, S. Rankin, A. R. Venkitaraman, S. Neidle, S. Balasubramanian, *Biochemistry* **2006**, 45, 7854-7860.

Graphical Abstract

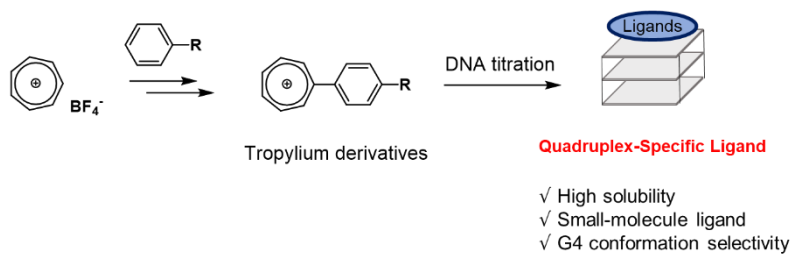
<Title> Tropylium Derivatives as New Entrants that Sense G-quadruplex Structures

<Authors' names> Daisuke Hori, Ji Hye Yum, Hiroshi Sugiyama*, and Soyoung Park*

<Summary>

Herein, we report G-quadruplex (G4) ligand candidates bearing a cationic tropylium skeletal structure. A set of tropylium derivatives were synthesized to generate a large π -conjugation system. Synthesized G4 ligand candidates displayed absorption peaks around 530 nm and different fluorescence depending on solvent conditions. Furthermore, we investigated their interactions with various DNA structures and found a strong interaction with G4s.

<Diagram>



Supporting Information

**Tropylium Derivatives as New Entrants that Sense
Quadruplex Structure**

Daisuke Hori^{1,‡}, Ji Hye Yum^{1,‡}, Hiroshi Sugiyama^{,1,2} and Soyoung Park^{*,1}*

¹Department of Chemistry, Graduate School of Science, Kyoto University, Kitashirakawa-
oiwakecho, Sakyo-ku, Kyoto 606-8502, Japan

²Institute for Integrated Cell-Material Sciences (iCeMS), Kyoto University, Yoshida-
ushinomiya-cho, Sakyo-ku, Kyoto 606-8501, Japan

**Corresponding author:* Dr. Soyoung Park, Prof. Dr. Hiroshi Sugiyama

Tel.: (+)81-75-753-4002; Fax: (+)81-75-753-3670

E-mail: oleesy@kuchem.kyoto-u.ac.jp, hs@kuchem.kyoto-u.ac.jp (H.S.)

Table of Contents

Materials	4
Methods and Equipment	4
Scheme S1. Synthetic Route of Tropylium Derivatives.....	5
Synthesis and characterization of Trop-AzP	5
Scheme S2. Synthetic scheme of 2d	5
Figure S1. N-phenylazetidide (2d).....	6
Figure S2. 1-(4-(cyclohepta-2,4,6-trien-1-yl)phenyl)azetidide (3d).....	6
Figure S3. Trop-AzP (4d).....	7
Oligonucleotide (ODN) Synthesis	8
Table S1. Analytical HPLC profile of synthesized ODNs.....	9
Table S2. MALDI-TOF-Mass data of ODNs.....	9
Solvatochromism of Tropylium Derivatives	10
Figure S4. UV-vis spectra of tropylium derivatives in various solvents.....	11
Figure S5. Fluorescent spectra of tropylium derivatives in various solvents.....	12
Figure S6. Fluorescent spectra of Trop-DEA excited at 570 nm (maximum absorption wavelength) in various solvents.....	13
Figure S7. Fluorescent spectra of Trop-DEA in the presence of c-kit G4 ^a	13
Figure S8. Solvent effect of tropylium derivatives observed by naked eyes ^a	14
UV titration	15
ITC Measurements	16
Figure S9. Isothermal titration calorimetry (ITC) measurements of DNAs and Trop-DEA ^a	17
Table S3. ITC parameters based on titration graph ^a	17
CD-Melting	18
Figure S10. Melting curves and T_m values of c-kit with and without derivatives ^a	19

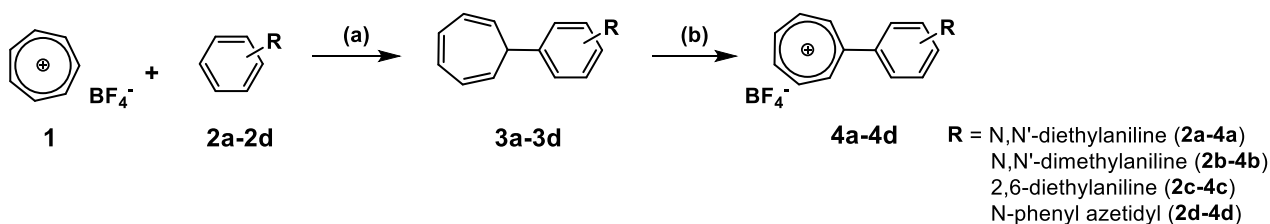
CD Spectroscopy	20
Figure S11. CD spectra of c-kit DNA with and without derivatives ^a	20
Figure S12. CD spectra of various DNA with 5 equivalent of derivatives ^a	21
Cytotoxicity	22
Figure S13. Cell viability assay results ^a	23
DFT Calculations	24
Figure S14. Energy-minimized structure of Trop-DEA.....	25
Figure S15. Energy-minimized structure of Trop-DMA.....	25
Figure S16. Energy-minimized structure of Trop-26DEA.....	25
Figure S17. Energy-minimized structure of Trop-AzP.....	25
Molecular Modeling study	26
Figure S18. Energy-minimized model between c-kit and Trop-DEA and Trop-26DEA.....	27
References	27

Materials

Tropylium tetrafluoroborate, dimethylaniline, diethylaniline, iodobenzene, tris(dibenzylideneacetone)-dipalladium (0), 4,5-bis(diphenylphosphino)-9,9-dimethylxanthene, and azetidine hydrochloride were received from TCI. Acetonitrile Superhydrated, sodium tert-butoxide, 1,4-dioxane and sodium hydroxide were received from Wako Chemicals and used without further purification. 2,6-diethylaniline was purchased from Sigma-Aldrich Chemicals Co. and used as received. Glen-Pak™ DNA and RNA cartridges columns were purchased at Glen Research. All other chemicals and solvents for DNA synthesis were purchased from Sigma-Aldrich Chemicals Co. and used without further purification. Water was deionized (specific resistance of ≥ 18.0 MW cm at 25°C) by a Milli-Q system (Millipore Corp.). All reactions were carried out under an argon atmosphere unless otherwise stated.

Methods and Equipment

NMR spectra were obtained on a JEOL JNM ECA-600 spectrometer operating at 600 MHz for ^1H NMR and 150 MHz for ^{13}C NMR in CDCl_3 unless otherwise noted. Flash column chromatography was performed employing Silica Gel 60 (70–230 mesh, Merck Chemicals). Silica-gel preparative thin-layer chromatography (PTLC) was performed using plates from Silica gel 70 PF₂₅₄ (Wako Pure Chemical Ind. Ltd.). DNA concentrations were measured by NanoDrop ND-1000 spectrophotometer. Stock 100 mM Na cacodylate buffer (pH 5.5, pH 7.0) and Tris-HCl buffer (pH 7.5) were prepared by dissolving sodium cacodylate trihydrate (1.07 g, 5.0 mmol) or trisaminomethane base (1.21 g, 5.0 mmol) in milliQ water (25 mL) before adjusting to the desired pH with hydrochloric acid and minimal sodium hydroxide, then topping up to 50 mL with milliQ water. Measurement of pH was conducted with a LAQUA F-72 pH/ion meter (HORIBA Ltd., Kyoto, Japan).

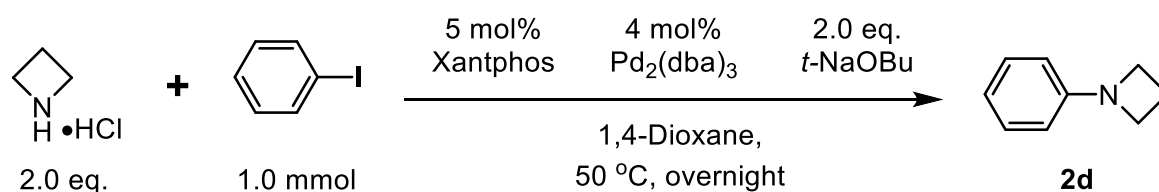


Scheme S1. Synthetic Route of Tropylium Derivatives

Reagents and conditions: (a) NaH, ACN, rt, overnight (yield: 80%); (b) Tropylium Tetrafluoroborate, ACN, rt, overnight (73%~quant)

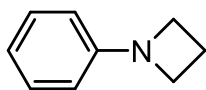
The detailed synthetic route and characterization data for Trop-DMA, Trop-DEA, and Trop-26DEA were reported by Nguyen T. V. and co-workers.^{S1} Newly synthesized tropylium derivative was prepared followed by same synthetic route.

Synthesis and characterization of Trop-AzP

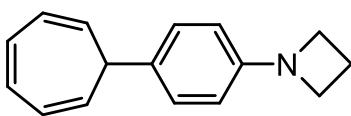


Scheme S2. Synthetic scheme of 2d

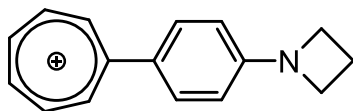
For the preparation of 1-phenylazetidine, azetidine hydrochloride and iodobenzene were coupled by Buchwald-Hartwig coupling reaction.^{S2} To a dry flask under an argon atmosphere was added azetidine hydrochloride (187 mg, 2.00 mmol, 2.0 equiv.), iodobenzene (115 μL , 1.0 mmol), Xantphos (29 mg, 0.05 mmol, 5 mol%), $\text{Pd}_2(\text{dba})_3$ (37 mg, 0.04 mmol, 4 mol%) and *t*-BuONa (192 mg, 2.00 mmol, 2.0 equiv). Then, anhydrous degassed 1,4-dioxane was added (15 mL) and the mixture was stirred at 50 $^\circ\text{C}$ for 1 day. Then, it was cooled to RT, brine (10 mL) and water (20 mL) were added and the mixture was extracted with Et_2O ($2 \times 50\text{ mL}$). Collected extracts were dried over Na_2SO_4 , filtered and evaporated. The target compound was obtained in good yield (50%). The subsequent p-conjugation of tropylium salt was performed followed by reported synthetic scheme.

**2d****Figure S1.** N-phenylazetidine (**2d**)

^1H NMR (CDCl_3): δ 7.21 (t, $J_{\text{HH}} = 7.1$ Hz, 2H), 6.73 (t, $J_{\text{HH}} = 6.7$ Hz, 1H), 6.46 (d, $J_{\text{HH}} = 6.8$ Hz, 2H), 3.87 (td, $J_{\text{HH}} = 7.1$ Hz, 2.5 Hz, 4H), 2.34 (quint, $J_{\text{HH}} = 3.74$ Hz, 2H). ^{13}C NMR (CDCl_3): δ 128.8, 128.6, 117.2, 111.3, 52.4, 16.9. HRMS (ESI-TOF) calculated for $\text{C}_9\text{H}_{12}\text{N}_1$ $[\text{M}+\text{H}]^+$ 134.0970, found 134.0962.

**3d****Figure S2.** 1-(4-(cyclohepta-2,4,6-trien-1-yl)phenyl)azetidine (**3d**)

^1H NMR (CDCl_3): δ 7.21 (d, $J_{\text{HH}} = 8.8$ Hz, 2H), 6.73 (t, $J_{\text{HH}} = 3.1$ Hz, 2H), 6.48 (d, $J_{\text{HH}} = 8.2$ Hz, 2H), 6.23 (d, $J_{\text{HH}} = 8.9$ Hz, 2H), 5.40 (dd, $J_{\text{HH}} = 9.5$ Hz, 5.5 Hz, 2H), 3.88 (t, $J_{\text{HH}} = 7.5$ Hz, 4H), 2.59 (t, $J_{\text{HH}} = 5.4$ Hz, 1H), 2.36 (quint, $J_{\text{HH}} = 7.1$ Hz, 2H). ^{13}C NMR (CDCl_3): δ 151.1, 132.6, 130.8, 127.9, 127.1, 123.9, 111.6, 52.6, 44.6, 16.9. HRMS (ESI-TOF) calculated for $\text{C}_{16}\text{H}_{18}\text{N}_1$ $[\text{M}+\text{H}]^+$ 224.1439, found 224.1426.

**4d****Figure S3.** Trop-AzP (**4d**)

^1H NMR (CD_3CN): δ 8.75 (d, $J_{\text{HH}} = 10.9$ Hz, 2H), 8.18 (quint, $J_{\text{HH}} = 5.1$ Hz, 2H), 8.07 (dd, $J_{\text{HH}} = 6.4$ Hz, 3.7 Hz, 2H), 7.98 (d, $J_{\text{HH}} = 9.7$ Hz, 2H), 6.96 (d, $J_{\text{HH}} = 9.5$ Hz, 2H), 3.74 (t, $J_{\text{HH}} = 7.1$ Hz, 4H), 2.36 (quint, $J_{\text{HH}} = 6.5$ Hz, 2H). ^{13}C NMR (CD_3CN): δ 154.9, 146.6, 145.5, 144.1, 133.3, 130.7, 124.7, 111.9, 59.4, 15.8. HRMS (ESI-TOF) calculated for $\text{C}_{16}\text{H}_{16}\text{N}^+$ $[\text{M}+\text{H}]^+$ 222.1277, found 222.1278.

Oligonucleotide (ODN) Synthesis

ODNs were synthesized on solid supports using commercially available O^5' -dimethoxytrityl -2'-deoxyribonucleoside O^3' -phosphoramidites. Solid-phase oligonucleotide synthesis was performed on an ABI DNA synthesizer (Applied Biosystem, Foster City, CA). Cleavage from the solid support and deprotection were accomplished with 50:50 of MeNH₂ in 40 wt. % in water and NH₃ in 28 wt. % in water at RT for 15 min and then at 65 °C for 15 min. The synthesized oligonucleotides were eluted from Glen-Pak™ DNA purification cartridges with purification steps are performed as per procedure. The final elution was subjected to normal-phase HPLC purification for the quality check. The products were confirmed by MALDI-TOF MS using a Bruker microflex-KSII (Bruker Corporation, Billerica, MA) (Table S2). DNA concentrations were determined by using NanoDrop ND-1000 (NanoDrop Technologies, Wilmington, DE).

For HPLC analysis, COSMOSIL 5C18 AR-II (Nacalai Tesque, Inc., Kyoto, 150 × 10 mm id), a linear gradient of 2 % to 30 % acetonitrile (in 20 mM TEAA (pH 7.0) buffer) over 30 min at a flow rate of 3.0 mL/min and detection at 254 nm were used.

Table S1. Analytical HPLC profile of synthesized ODNs



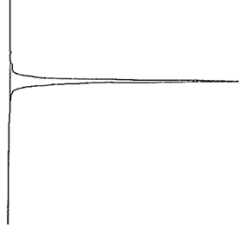
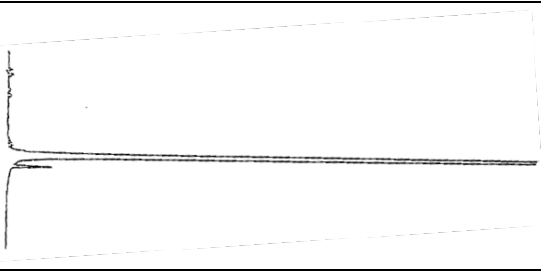
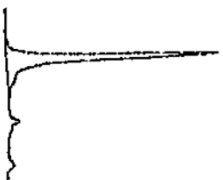
ODN	HPLC Profile	
Duplex	11.225	
i-motif	14.600	
TTAG ₄	11.933	
HT22	12.567	
c-kit	13.542	

Table S2. MALDI-TOF-Mass data of ODNs

Name	DNA oligomers	Calcd.	Found
Duplex	GGACCGCGGTCC	3647.37	3645.08
i-motif	CCCTTACCCTTACCCTACCC	6173.00	6174.65
TTAG ₄	TTAGGGG	2176.45	2175.07
HT22	AGGGTTAGGGTTAGGGTTAGGG	6966.49	6968.66
c-kit	AGGGAGGGCGCTGGGAGGAGGG	7011.50	7013.65

Solvatochromism of Tropylium Derivatives

Synthesized Tropylium derivatives (known and newly synthesized one) were prepared as stock solution (5 mM in DMSO). For spectroscopic studies, samples were prepared by dissolved to various solvent (MeOH, mQ, Acetonitrile, Ethyl acetate, Dichloromethane, Dichloroethane) or acetonitrile in the presence of 1.0 equivalent of TBAF, TBAC, TBAB or TBAI to 50 μ M. UV-vis absorbance spectra were measured from 220 nm to 700 nm at 20 °C on a JASCO V-750 spectrophotometer equipped with a JASCO PAC-743R thermocontrolled cell changer and a JASCO CTU-100 thermocirculator. All samples were prepared in a total volume of 120 μ L (final concentration 100 μ M). And, fluorescence measurements were obtained using 3 mm path length JASCO FMM-100 quartz microcells on a JASCO FP-6300 Spectrofluorometer equipped with a JASCO EHC-573 temperature controller. The emission spectra were recorded from 220 nm to 700 nm at a scan rate of 500 nm/min with an excitation wavelength of 365 nm. Images of compounds were obtained with a Nikon 3100 DSLR camera attached with a 75-200 mm lens, or iphone S7.

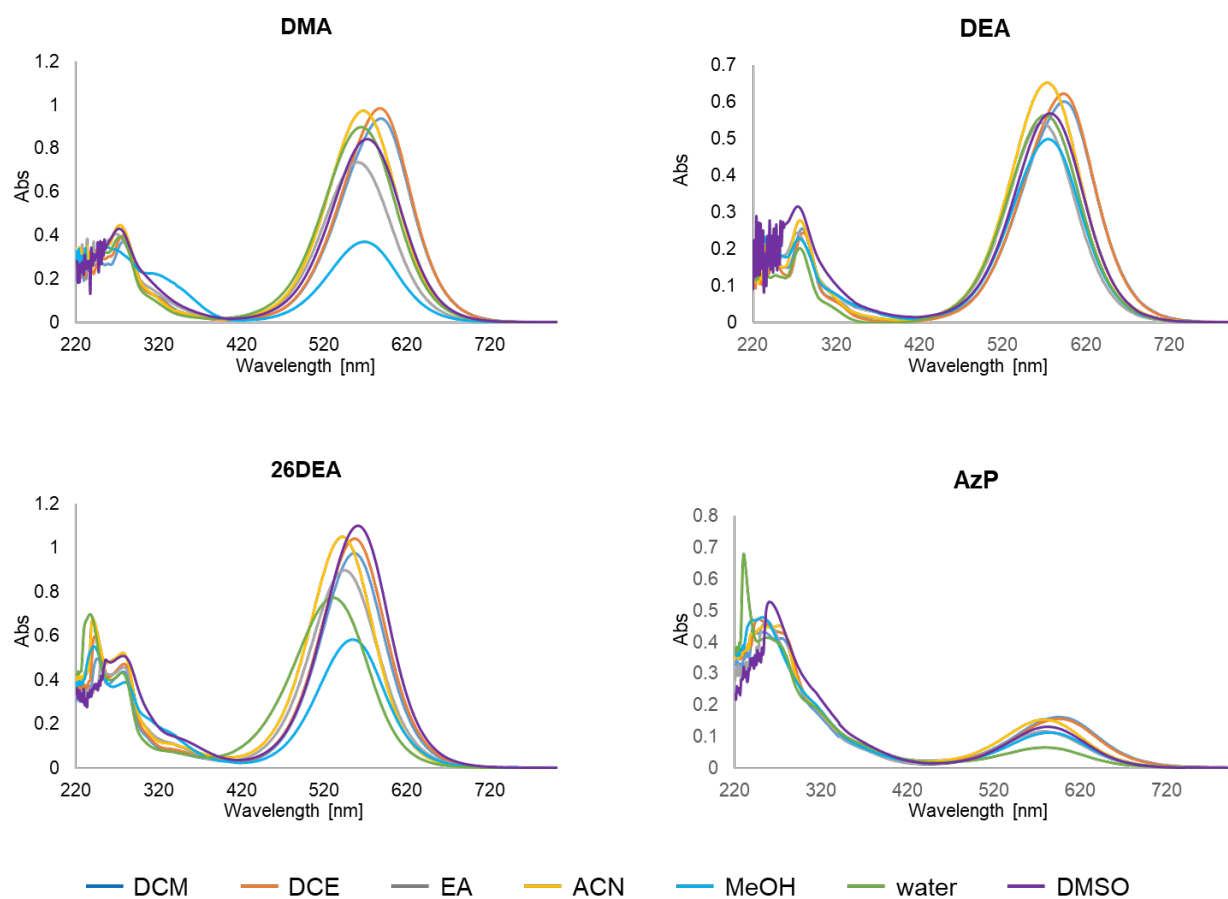


Figure S4. UV-vis spectra of tropylium derivatives in various solvents

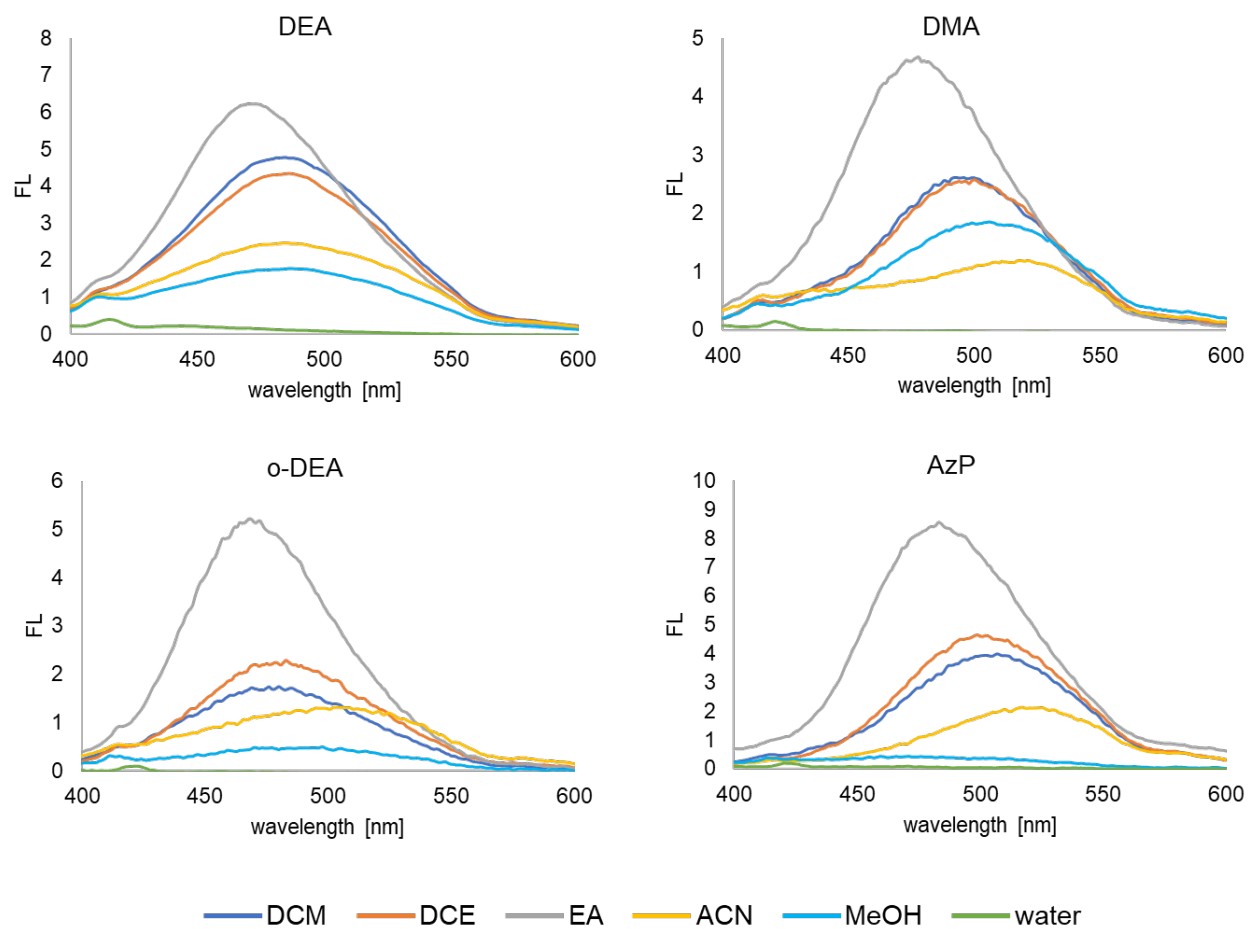


Figure S5. Fluorescent spectra of tropylium derivatives in various solvents

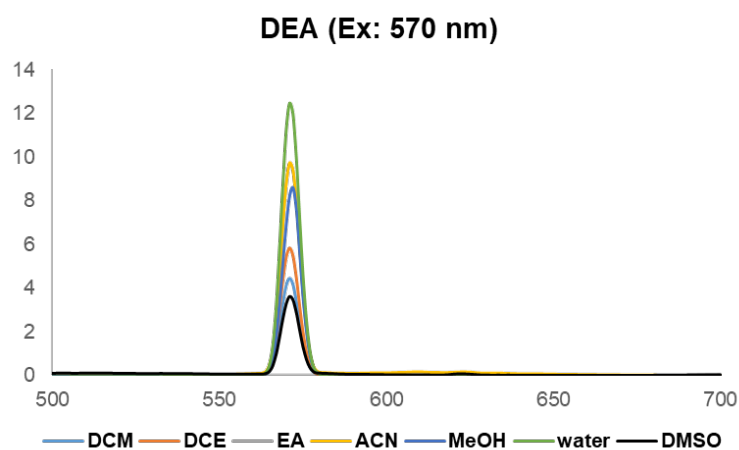


Figure S6. Fluorescent spectra of Trop-DEA excited at 570 nm (maximum absorption wavelength) in various solvents

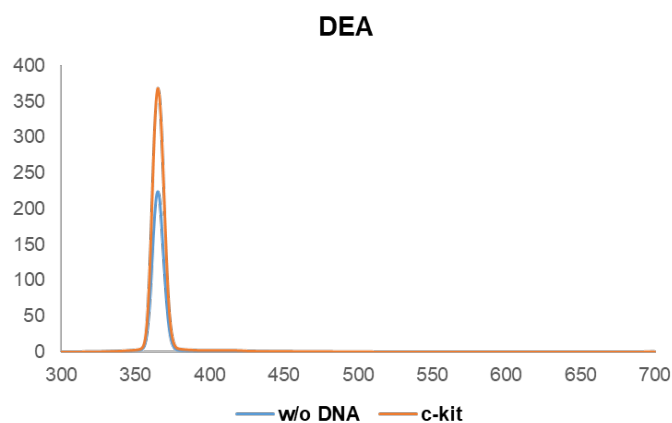


Figure S7. Fluorescent spectra of Trop-DEA in the presence of c-kit G4 ^a

^a Solution conditions: 100 μ M Trop-DEA in 10 mM Na cacodylate buffer (pH 7.0) and 50 mM KCl, the presence and absence of 1 equiv. of pre-structured c-kit G4 DNA.

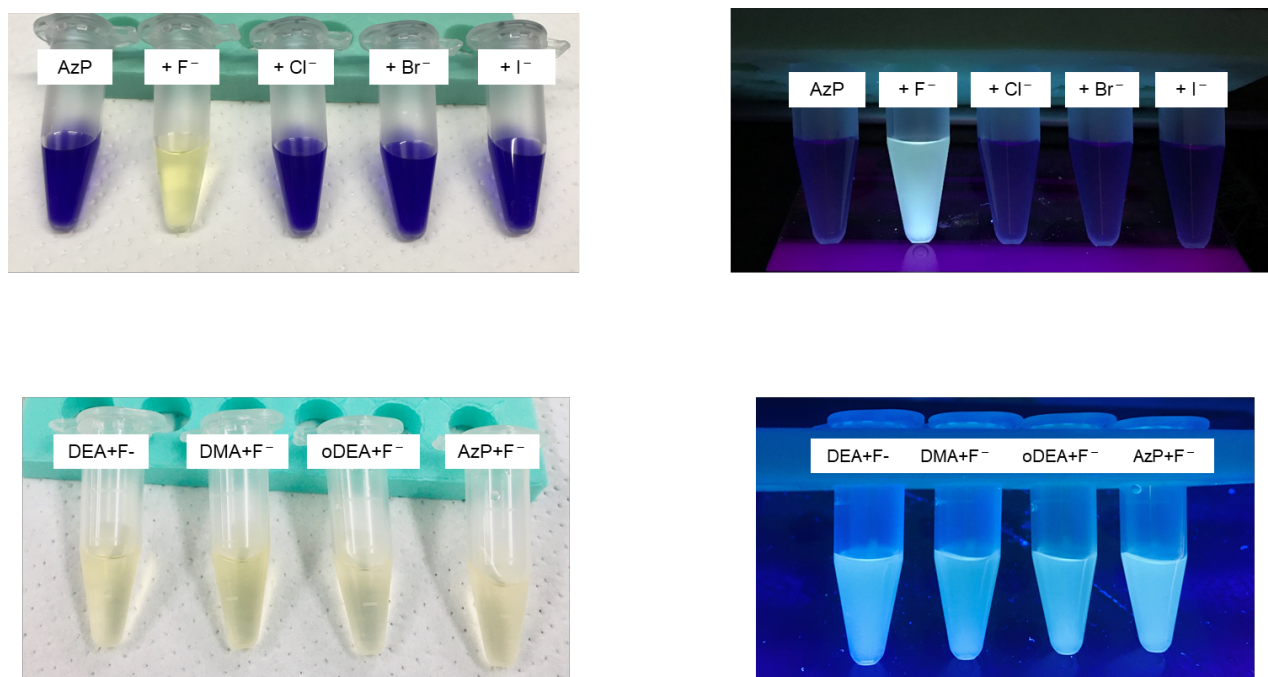


Figure S8. Solvent effect of tropylium derivatives observed by naked eyes ^a

^a 150 μ M of tropylium derivatives and 1 equiv. of TBAX (here, X = F, Cl, Br, and I) in 500 μ L ACN.

UV titration

Binding assays were performed with preformed duplex DNA [d(GGACCGCGGTCC)] in 20 mM Na cacodylate (pH 7.0), with 100 mM NaCl, i-motif DNA [d(CCCTTACCCTTACCCTTACCC)] in 20 mM Na cacodylate (pH 5.5), and for G-quadruplex DNA sets in 20 mM Tris-HCl (pH 7.5) with 100 mM KCl. All of the oligonucleotides were dissolved in required buffer at the indicated concentration. The solution was first heated to 95 °C for 5 min and then cooled slowly to room temperature over a period of 6 h. The ligand solution (50 μM, 500 μL) was titrated by stepwise addition of aliquots of the DNA solution (1.5 mM). After each addition, the mixture was incubated at 20 °C for 5 min before measurement. Molar absorptivity (Abs/10 μM) was calculated for the comparison. The fractional decrease in absorbance at each maximum wavelength was plotted as dot graph to estimate the binding equivalents.

ITC Measurements

ITC experiments were performed on secondary structured DNAs using a MicroCal™ iTC200 isothermal titration calorimeter courtesy by Prof. Takashi Morii and Dr. Eiji Nakata. After several concentration optimizations for the titration saturations, the titration of 2 mM Trop-DEA on 10 μ M duplex, c-kit G4, and i-motif DNAs was carried out in buffers for secondary structural formation at 25 °C. The titrations were conducted in time interval as 180 s, cell temperature 25°C, reference power 5 μ cal/sec. initial delay 60 sec, stirring speed 1000 rpm, and the injection volume was 2.0 μ L after 4 sec durations. Before initiating automatic titration, the temperature and baseline is fully stabilized over 30 min. The reference cell contained distilled and deionized water. Before the experiment, the samples were heated at 95 °C, 5 min then slowly cooled down to RT (1 °C min⁻¹). The data were analyzed using Origin 7.0 (Microcal software) with an automatically generated baseline fixing ligand binding number (N) as 2.

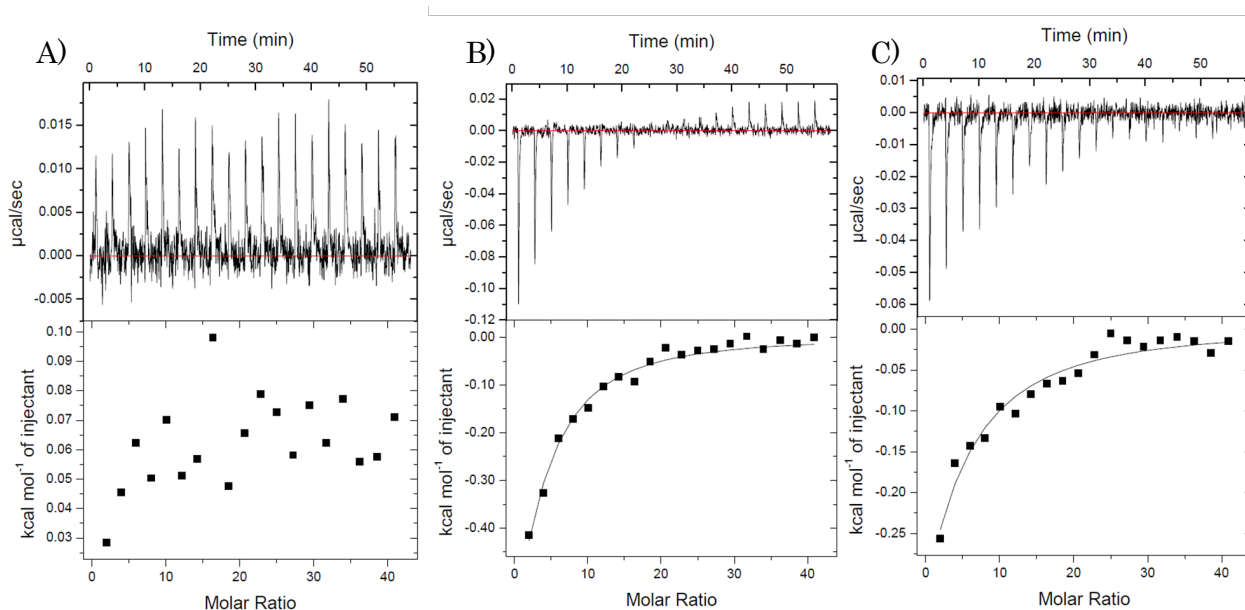


Figure S9. Isothermal titration calorimetry (ITC) measurements of DNAs and Trop-DEA ^a

^a Solution conditions: 10 μM DNAs are titrated with 2 mM of Trop-DEA in adjusted solvent conditions.

(A) ITC profiles of duplex DNA in 10 mM Na Cacodylate buffer (pH 7.0) with 50 mM NaCl and 2 mM ligand; (B) ITC profiles of i-motif DNA in 10 mM Na Cacodylate buffer (pH 5.5) and 2 mM ligand; (C) ITC profiles of c-kit G4 in 10 mM Na Cacodylate buffer (pH 7.0) with 50 mM KCl and 2 mM ligand.

Table S3. ITC parameters based on titration graph ^a

^a Solution conditions: 10 μM DNAs are titrated with 2 mM of Trop-DEA in identical solvent conditions.

DNA	ΔH (kcal/mol)	TAS (kcal/mol)	K (/M)	ΔG (kcal/mol)	N (fixed)
i-motif	-2.3 ± 0.09	3.3	$(14.2 \pm 1.1) \times 10^3$	-5.6	2
c-kit G4	-1.9 ± 0.10	3.4	$(8.7 \pm 1.0) \times 10^3$	-5.3	2
duplex	No binding is observed				

CD-Melting

CD spectra of oligonucleotide solutions collected in 0.5-nm steps from 350 to 220 nm were measured using JASCO J-805LST Spectrometer in a 1-cm quartz cuvette. Ellipticity was recorded in the forward direction at temperatures from 20 to 95 °C at a rate of 1.0 °C/min and each spectrum shown is the average of two individual scans. The melting samples were denatured at 95 °C for 5 min and annealed slowly to RT. All melting samples were prepared in a total volume of 150 μ l containing 4 μ M of each strand oligonucleotide, various equivalent of tropylium derivatives, 10 mM Na Cacodylate buffer (pH 7.0) and 1 mM KCl.

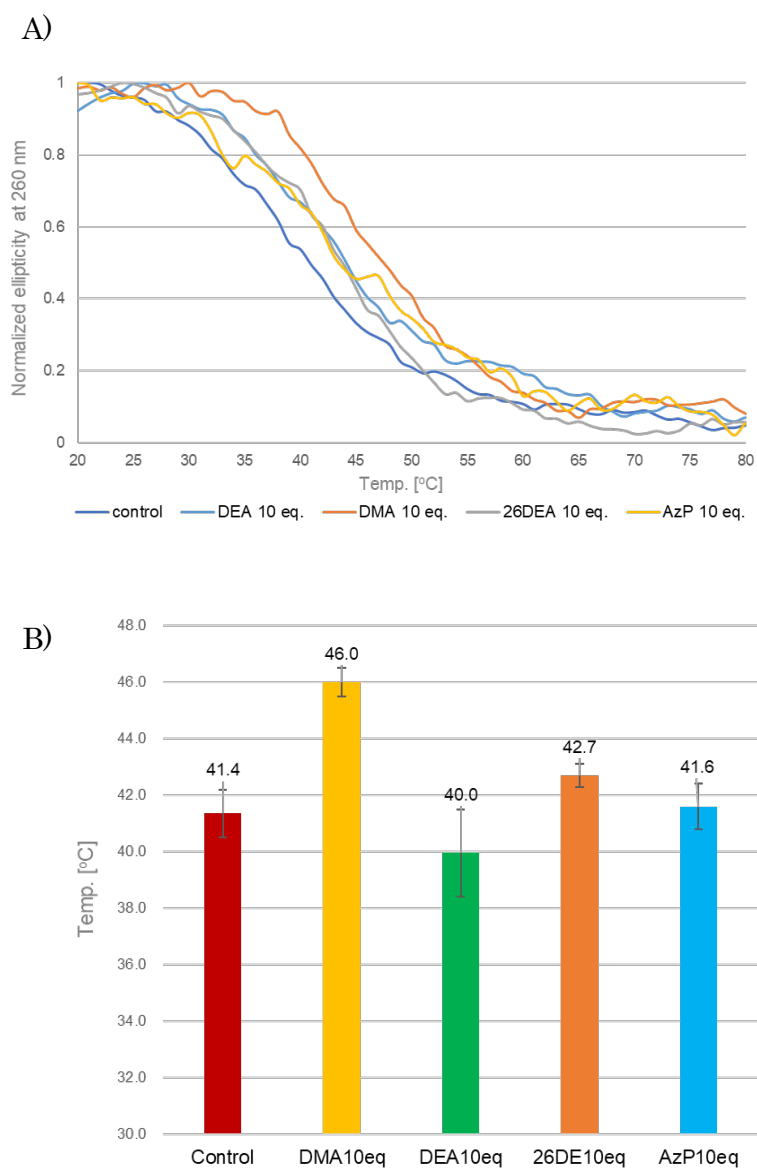


Figure S10. Melting curves and T_m values of c-kit with and without derivatives ^a

^a Solution conditions: 4 μ M DNA in 10 mM Na Cacodylate buffer (pH 7.0) and 1 mM KCl, the presence and absence of tropylium derivatives.

(A) Representative CD-melting curve of c-kit; (B) T_m values.

CD Spectroscopy

CD spectra of oligonucleotide solutions collected in 1 nm steps from 360 nm to 220 nm were measured using JASCO J-805LST Spectrometer in a 1 cm quartz cuvette. Each spectrum shown is the average of two individual scans. The samples were denatured at 95 °C for 5 min and annealed slowly to RT until experiments were initiated. All melting samples were prepared in a total volume of 120 μL containing 4 μM oligonucleotide in the presence of identical equivalent of tropylium derivatives under certain secondary structure forming conditions.

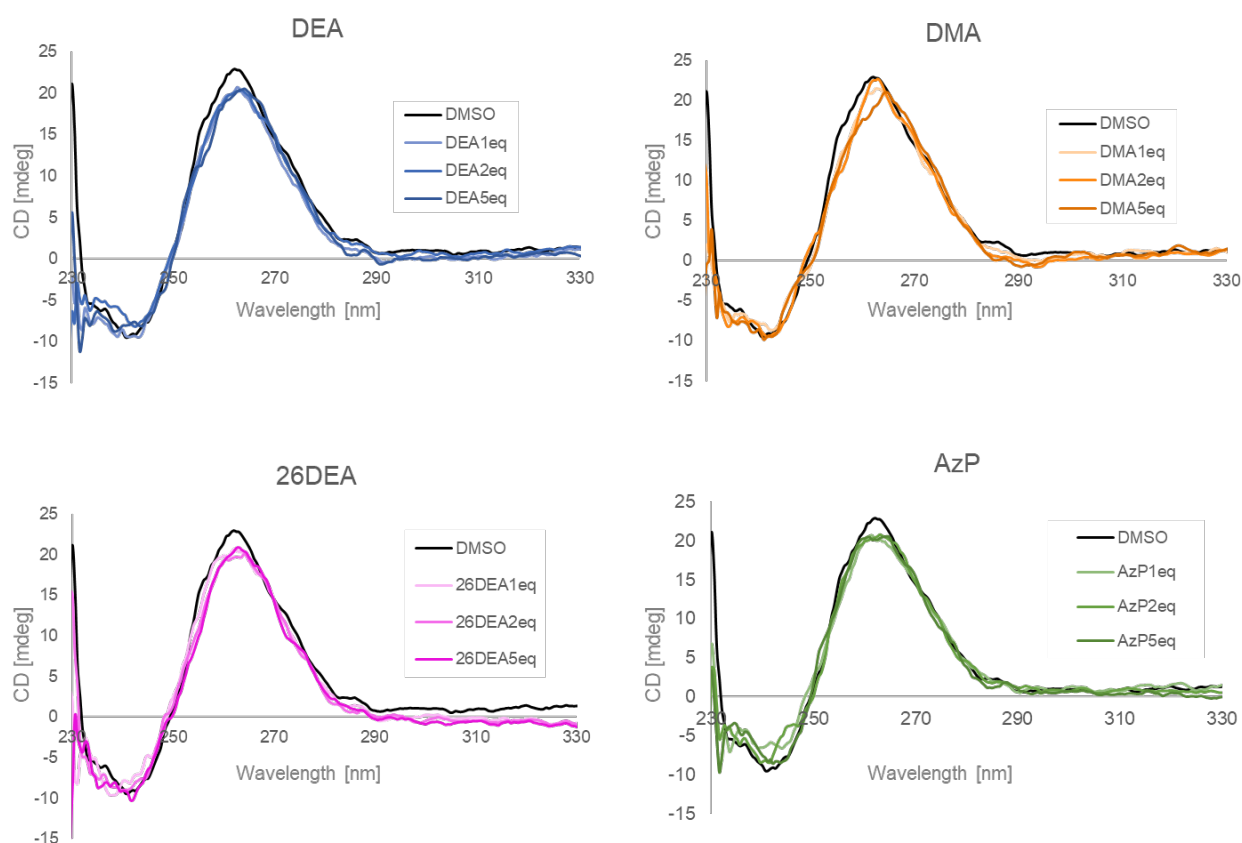


Figure S11. CD spectra of c-kit DNA with and without derivatives ^a

^a Solution conditions: 4 μM DNA in 10 mM Na cacodylate buffer (pH 7.0) and 1 mM KCl, the presence and absence of 1, 2 or 5 equiv. of tropylium derivatives.

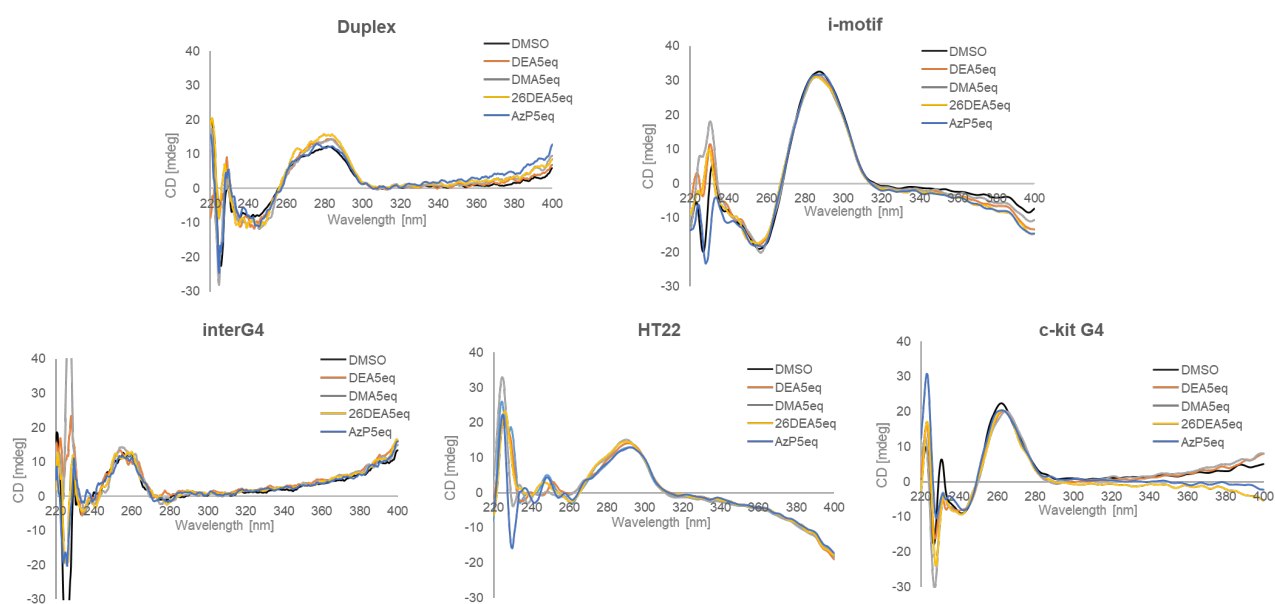


Figure S12. CD spectra of various DNA with 5 equivalents of derivatives ^a

^a Solution conditions: 4 μ M DNA in 10 mM Na cacodylate buffer (pH 7.0, pH 5.5 for i-motif DNA) and 1 mM NaCl (KCl for G4 forming sequences), the presence and absence of 5 equiv. of tropylium derivatives.

Cytotoxicity

Cultured HeLa cell was purchased from ATCC and maintained in DMEM (Thermo Fisher Scientific) supplemented with 10 % (v/v) fetal bovine serum (FBS, Sigma Aldrich) at 37 °C with 5% CO₂. For the compound treatment, the cells were seeded on 96 well plate (ca. 5000 cells). Cultures were maintained at 37 °C in a humidified atmosphere containing 5% CO₂. After 2 days incubations for cell adhesions, cells were incubated for overnight with the tropylium derivatives (Trop-DEA, Trop-26DEA, and Trop-AzP) at 10 μM, 1 μM, and 0.1 μM (0.5% v/v). Wells containing 0.5% (v/v) DMSO cells were used as control. At the end of incubation, Cell Count Reagent SF (from nacalai tesque) was added to cell culture medium 10% (v/v) and left 1 hour at 37 °C. Finally, the absorbance was recorded in a SpectraMax M2 microplate reader (from Molecular Devices) at 450 nm. Cell viability relatively to control was expressed as mean ± SEM from at least three different experiments.

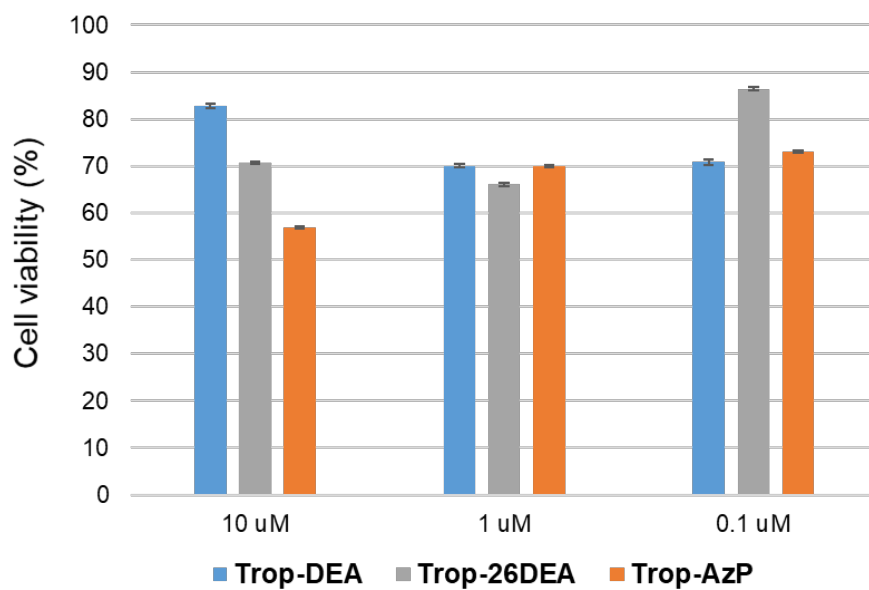


Figure S13. Cell viability assay results ^a

^a Cell viability of control (DMSO treated cells) is referred as 100%

DFT Calculations

The geometry of tropylium derivatives are optimized using DFT, and their optical spectra are calculated using DFT methods as implemented in the Gaussian 16W program package. All the calculations are done using B3LYP (Becke, three-parameter, Lee–Yang–Parr) hybrid exchange and correlation energy functional, default spin, with the 6-311G+(d,p) basis set for all atoms. The DFT calculations are performed both in the gas phase. After geometry optimization, frequency calculations are done to remove any vibrational unstable mode.

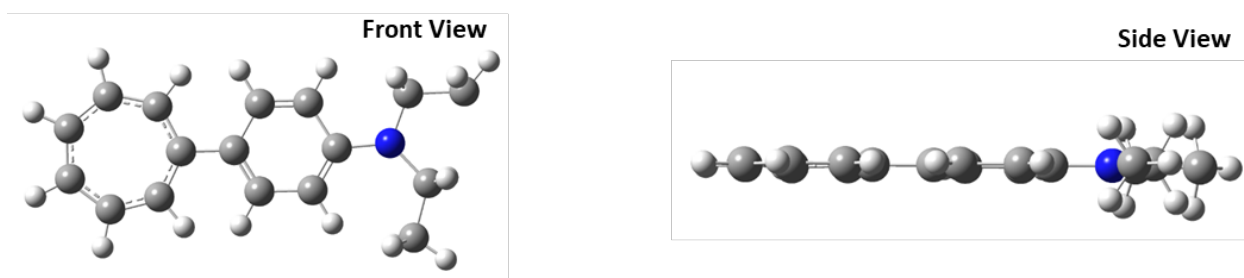


Figure S14. Energy-minimized structure of Trop-DEA.

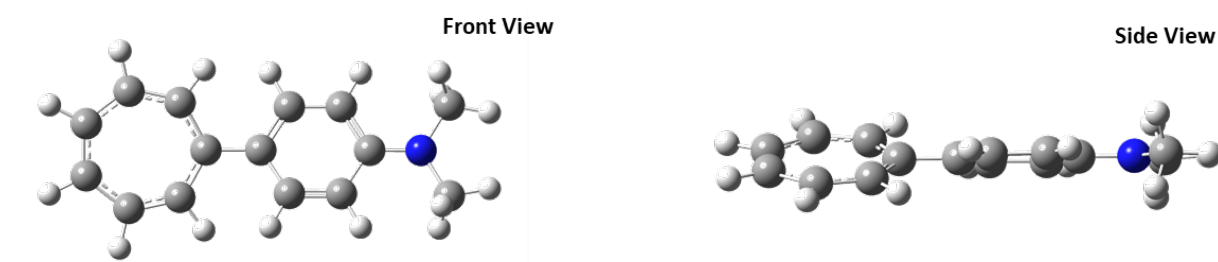


Figure S15. Energy-minimized structure of Trop-DMA.

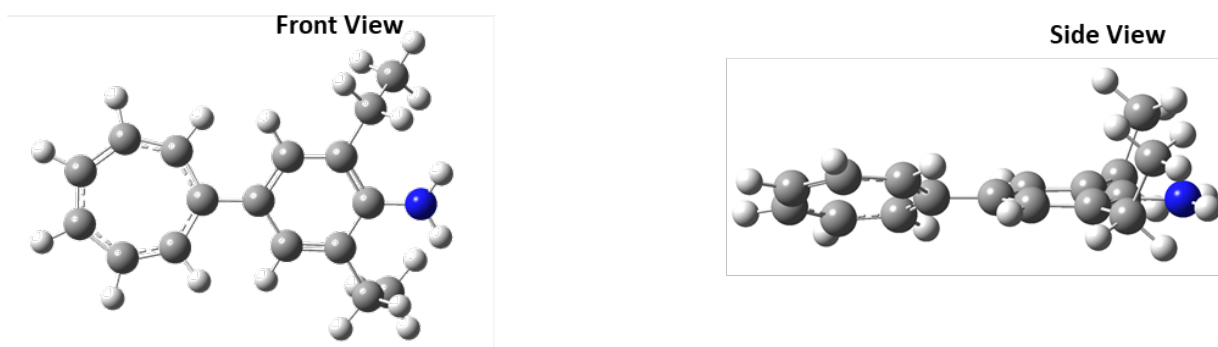


Figure S16. Energy-minimized structure of Trop-26DEA.

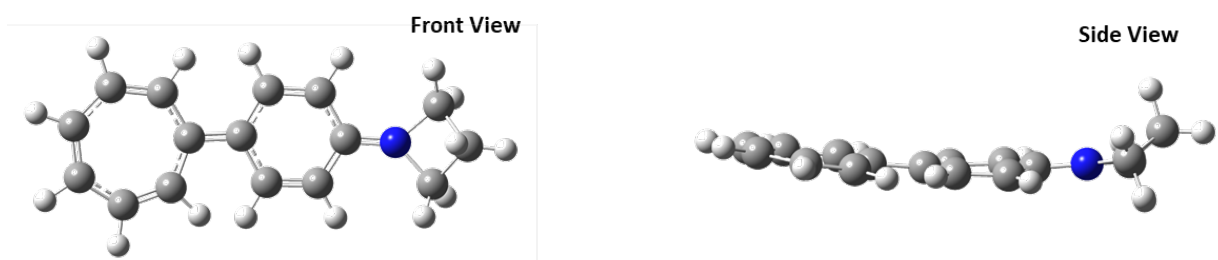


Figure S17. Energy-minimized structure of Trop-AzP.

Molecular Modeling study

Molecular modeling was carried out using the DS (Discovery Studio Client 2019) software package.

The c-kit G-quadruplex DNA has prepared base on previously reported crystal structure (PDB ID:

2O3M). The DFT calculation results of tropylium derivatives were positioned to the designated G-

quartet of c-kit (2:1=Ligand:DNA). For the construction of environment components before the

minimization, we chose Explicit Periodic Boundary as a solvation model. The shape of the water

and salt (0.1 M KCl) is orthorhombic with 10 Å minimum distance. Minimizations (RMS Gradient

to be 0.001) were operated for each model with CHARMM force field parameters. The obtained

structures were shown as Figure S12.

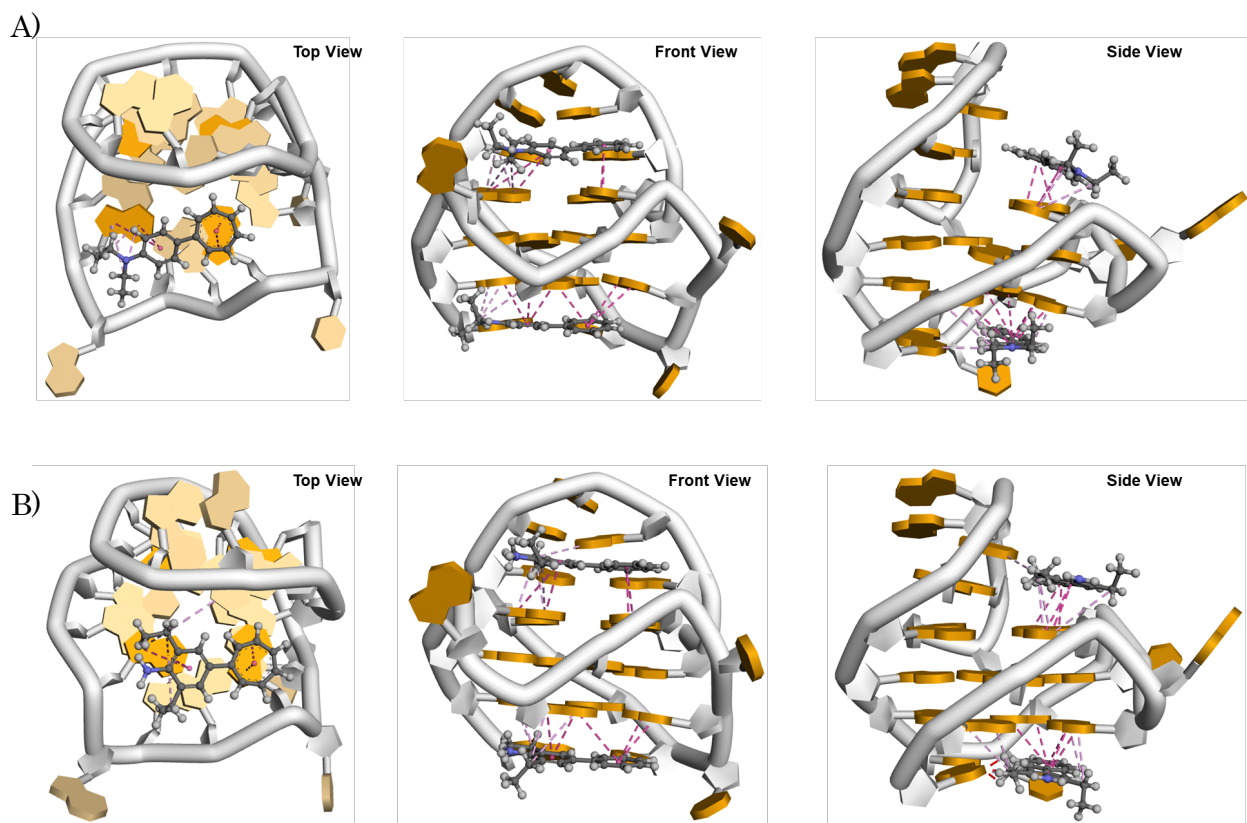


Figure S18. Energy-minimized model between c-kit and Trop-DEA and Trop-26DEA

^a Dot lines for non-covalent bonds including hydrophobic and electrostatic interactions.

(A) Energy minimized model between c-kit DNA and Trop-DEA, (B) Energy minimized model between c-kit DNA and Trop-26DEA.

References

- S1) Nguyen, T. V. Stimuli-Responsive Organic Dyes with Tropylium Chromophore. *Chem. Eur. J.* **2018**, *24*(43), 10959–10965.
- S2) Siegl, S. J., Galeta, J., Dzajak, R., Vázquez, A., Del Río-Villanueva, M., Dračínský, M., & Vrabec, M. An Extended Approach for the Development of Fluorogenic trans-Cyclooctene–Tetrazine Cycloadditions. *ChemBioChem*, **2019**, *20*(7), 886–890.